ChemComm

COMMUNICATION

View Article Online
View Journal | View Issue

Cite this: *Chem. Commun.*, 2023, 59, 6905

Received 5th April 2023,
Accepted 11th May 2023

DOI: 10.1039/d3cc01674a

rsc.li/chemcomm

The emission efficiency of cationic solid state luminophores is directly proportional to the intermolecular charge transfer intensity†

Kaspars Leduskrasts, Artis Kinens and Edgars Suna *

Cationic luminophores have recently emerged as a class of efficient emitters in both the solid state and solutions. However, the underlying processes that secure the emission in these luminophores are poorly understood. Here, we employ charge transfer integral (CTI) analysis in combination with X-ray single crystal data to uncover the emission mechanism in a series of pyridinium luminophores. We demonstrate that the solid state photoluminescence quantum yield (Φ) of cationic luminophores is directly proportional to the charge transfer (CT) intensity within a network of molecules in the crystal lattice. Electrostatic intermolecular interactions between π^+-systems in the crystal lattice provide a disproportionately high contribution to the CT intensity and therefore are instrumental in achieving high Φ. In addition, the strength of electrostatic interactions can be increased by a through-space (TS) electron-donation strategy. Hence, electrostatic interactions can be utilized as a tool to achieve radiative CT, which is useful in the development of efficient luminophores, sensors and nonlinear optical materials.

Light emitting molecules (luminophores) are key components in various modern technological applications, such as organic light emitting diodes,[1] light emitting electrochemical cells,[2] organic photovoltaics,[3] organic field effect transistors[4] and sensors.[5] Recent advances in luminophore design have rendered purely organic luminophores competitive or even superior to their inorganic or organometallic counterparts.[6] Generally, purely organic luminophores comprise neutral π systems (*e.g.* phenyl or naphthyl rings)[6b,7] and/or charged heteroaromatic subunits (π^+-systems such as imidazolium or pyridinium (Py^+) cations).[8] Luminophores designed exclusively from π-systems are highly efficient in solution; however, they typically lose emission effectiveness in the solid state (SS).[9] In contrast, the incorporation of a charged π^+-system into a luminophore renders it highly emissive in the SS.[8b,10] In particular, Py^+-containing luminophores have demonstrated dual emission,[11] aggregation induced emission (AIE)[8,10,12] and thermally activated delayed fluorescence (TADF) behavior.[13] Notably, charged π^+-system-containing emitters display high emission efficiency also in solution[14] and have found applications in sensing of alkylating reagents[15] as well as reversible solid[10c] and solution state[16] sensing of acids.

The high emission intensity of Py^+-derived luminophores both in solution and the SS has been attributed to the formation of *intermolecular* electrostatic π^+–π^{17} and π^+–π^+ interactions.[8b,10a,b,15] However, the light emission mechanism associated with these electrostatic interactions is still poorly understood. We and others have demonstrated recently that the intermolecular π^+–π interactions generate TS charge transfer (TSCT) bands in the crystal state.[8b,11] In this study we offer quantitative means to evaluate CT intensity in a crystal lattice by calculating the total electronic coupling ($\Sigma|V|$) value between the luminophores as described below. We have also shown that that π^+–π^+ interactions significantly increase $\Sigma|V|$ and enhance the SS photoluminescence quantum yields (Φ).

To unravel the role of the π^+–π^+ interactions in SS emission, we elected to modify a previously published Py^+ luminophore **1**.[10a] Specifically, a series of **1** analogues with the benzyl Py^+ subunit *ortho* to the carbazole (**2**), 3,6-dimethylcarbazole (**3**) and 3,6-di-*tert*-butylcarbazole (**4**) substituents was prepared with mesylate (**2a**, **3**), chloride (**2b**, **4a**) and perchlorate (**4b**) as the counter ions (Fig. 1 and 2). We envisioned that **2**–**4** should be capable of forming key π^+–π^+ interactions in the SS similar to parent **1**. We also hypothesized that placing the benzyl Py^+ subunit in close spatial proximity[18] to the carbazole ring could lead to a TS electron donation from the carbazole to the Py^+ moiety and further enhance the strength of the *intermolecular* π^+–π^+ interactions in **2**–**4**.

UV-Vis spectra for Py^+ salts **2**–**4** were measured in MeCN solutions at room temperature and under ambient atmosphere at *ca.* 10^{-5} M concentration (see ESI,† pages S11–S16). The previously published Py^+ salt **1** and the newly synthesized

Latvian Institute of Organic Synthesis, Aizkraukles 21, LV-1006, Riga, Latvia. E-mail: edgars@osi.lv

† Electronic supplementary information (ESI) available. CCDC 2216260, 2216261, 2247114, 2247115, and 2247116. For ESI and crystallographic data in CIF or other electronic format see DOI: https://doi.org/10.1039/d3cc01674a

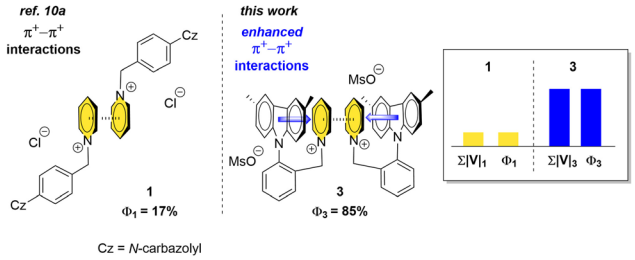

Fig. 1 Effect of enhanced π^+–π^+ interactions on Φ and $\Sigma|V|$.

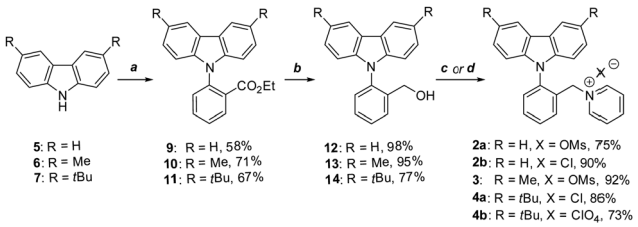

Fig. 2 Synthesis of Py^+ salts **2**–**4**. Reagents and conditions: (a) ethyl 2-bromobenzoate (**8**, 1.2 or 1.3 equiv.), CuI (15 mol%), L-proline (30 mol%), K_2CO_3, and DMSO, at 140 °C, for 72 h, and a 58% yield for **9**; 71% for **10**; and 67% for **11**. (b) $LiAlH_4$, THF, at 70 °C, for 1 h, and a 98% yield for **12**; 95% for **13**; and 77% for **14**. (c) MsCl, DIPEA, and DCM, at 0 °C to rt, for 1 h, then pyridine, MeCN, for 72 h, and a 75% yield for **2a**; 92% for **3**. (d) Conditions (c) followed by reversed-phase chromatography, containing aqueous HCl as a mobile phase, a 90% yield for **2b**, and an 86% yield for **4a**; alternatively aqueous $HClO_4$ as a mobile phase, 73% yield for **4b**.

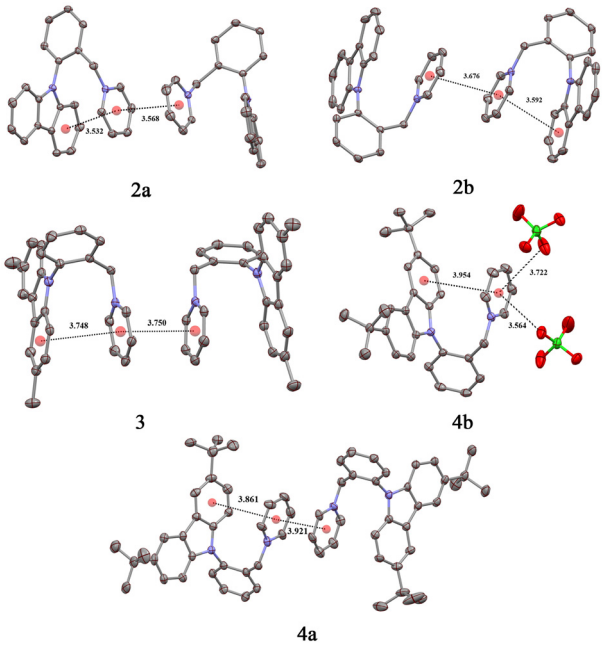

Fig. 3 X-Ray representations of **2**–**4**.

luminophores **2**–**4** featured four absorption bands at 238–241, 289–294, 321–333 and 334–345 nm (Table 1). Py^+ salts **2**–**4** displayed negligible emission in MeCN solutions with Φ values below 0.1% and emission peaks at 344–357, 352–373 and 597–606 nm. The emission at 340–380 nm was attributed to the locally excited states, while the extremely broad and weak emission at around 600 nm was attributed to the intramolecular TSCT between the carbazole and Py^+ moieties in solution. In the solid state, **2**–**4** displayed intense emission with maxima in the 437–490 nm range (see ESI,† pageS S17–S19). Notably, Py^+ salts **2a**, **2b**, **3** and **4a** showed considerably higher SS Φ (43.5, 35.0, 85.2, and 42.3%, respectively), as compared to the published analog **1** (17.3%). Obviously, placement of the benzyl Py^+ moiety in close proximity to the carbazole subunit affected strongly the AIE properties of Py^+ luminophores.

X-Ray crystallography was employed to analyze the mutual orientation of the proximate carbazole and Py^+ moieties in the crystal lattices of emitters **2**–**4**.[19] Crystals of **2a**, **2b**, **3** and **4a** suitable for X-ray analyses were obtained by Et_2O vapor diffusion into their MeCN solutions, while crystallization from water was required for **4b**. The emitters crystallized as monoclinic (**2a**, **2b**, and **4a**), triclinic (**3**), and orthorhombic (**4b**) colorless plates (**2a**, **4b**) and prisms (**2b**, **3**, and **4a**) with $P2_1/c$ (**2a**, **2b**), $P\bar{1}$ (**3**), $P2_1/n$ (**4a**) and *Pbca* (**4b**) space groups. As anticipated, relatively short distances between neighboring Py^+ moieties in the crystal lattices of **2a** (3.568 Å), **2b** (3.676 Å), **3** (3.750 Å) and **4a** (3.921 Å) were observed, indicating the presence of intermolecular π^+–π^+ interactions. However, **4b** did not possess close inter-pyridinium contacts. Instead, the Py^+ moiety in **4b** was engaged in interactions with two perchlorate counter ions as evidenced by the relatively close 3.564 and 3.722 Å distances between the Py^+ centroid and the respective oxygen atoms. The lack of SS π^+–π^+ interactions in **4b** is obviously responsible for reduced SS Φ as compared to all other *ortho*-substituted Py^+ salts (**2a**, **2b**, **3**, and **4a**). This observation provides strong evidence for the importance of π^+–π^+ interactions in SS emission of **2**–**4**. In the meantime, the large difference in Φ between *ortho*-substituted luminophores **2a**, **2b**, **3** and **4a**, and parent emitter **1** suggested an involvement of additional favorable interactions in the crystal lattices of **2a**, **2b**, **3** and **4a**. Indeed, a close distance

Table 1 Photoluminescence properties of luminophores **1**–**4**

Entry	Compound	λ_{abs}, nm	Solution λ_{em}, nm	Solid λ_{em}, nm	Solution, Φ (%)	Solid, Φ (%)
1	**1**	241, 290, 325, 337	—	505	<0.1	17.3
2	**2a**	238, 289, 321, 334	344, 360, 606	490	<0.1	43.5
3	**2b**	241, 289, 322, 334	352, 597	473	<0.1	35.0
4	**3**	241, 296, 333, 345	357, 373, 602	488	<0.1	85.2
5	**4a**	240, 294, 328, 340	355, 370, 560	463, 480	<0.1	42.3
6	**4b**	241, 294, 328, 340	355, 370, 575	437	<0.1	19.1

between the carbazole and Py^+ moieties was also measured for **2a** (3.532 Å), **2b** (3.592 Å), **3** (3.748 Å), and **4a** (3.861 Å; see Fig. 3). Apparently, the superior Φ values for **2a**, **2b**, **3**, and **4a** as compared to **1** are to be attributed to enhancement of the key intramolecular π^+–π^+ interactions by the TS electron donation from the carbazole moiety to the Py^+ ring.

The observed drop in SS Φ in the absence of intermolecular π^+–π^+ interactions for **4b** indicated that an intermolecular process such as CT[20] may play a key role in the mechanism of the SS emission for **1–4**. The enhanced strength of the π^+–π^+ interactions in the crystalline framework should increase the electronic communication between luminophores, which can be approximated by the electronic coupling value V.[21] V is widely utilized for quantifying short range CT for holes and electrons[22] by evaluating the HOMO–HOMO and LUMO–LUMO overlaps between neighboring luminophores. Accordingly, we performed a thorough CT integral (CTI) analysis for crystal state emitters **1–4** (see ESI,† pageS S25–S34). All possible CT pathways (CTPs) between a luminophore and all adjacent molecules in the crystal lattice were analyzed for both electron (blue vectors) and hole (red vectors) transfers (Fig. 4A) by Gaussian 09 and CATNIP[23] software using geometries obtained from X-ray data.

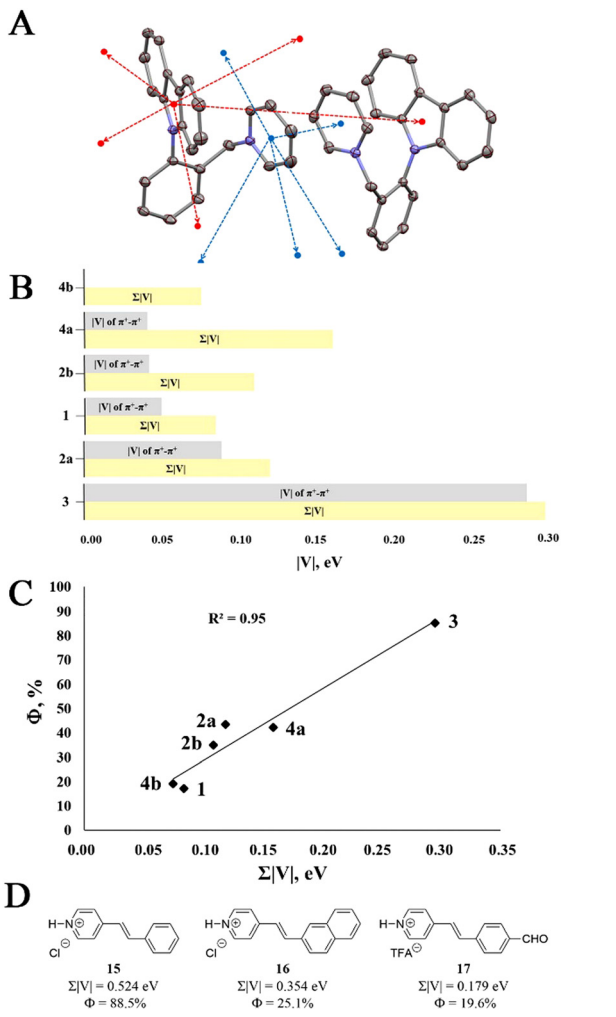

Fig. 4 (A) Hole and electron CTPs for **2a**. (B) Contribution of π^+–π^+ interaction-associated electronic coupling to the total sum of $|V|$ ($\Sigma|V|$). (C) Correlation between Φ and $\Sigma|V|$ in **1–4**. (D) CTI analysis of known luminophores **15–17**.

Perchlorate, chloride and mesylate counter ions in **1–4** were disregarded in the CTI calculations. Thus, it is well known that perchlorates do not form a CT complex with Py^+ ions.[24] Furthermore, the formation of a CT complex between an anion and a Py^+ ion would generate a new CT absorption band (CTAB) both in solution[25] and the SS,[26] resulting in colored solutions and solid materials. However, both mesylates **2a**, **3** and chlorides **2b**, **4a** form a colorless solution in MeCN and their absorption spectra are similar to that of the perchlorate **4b**. In contrast, the addition of TBAI as an iodide source to the colorless solution of perchlorate **4b** in EtOAc afforded a yellow-colored solution and the appearance of a new CTAB red-shifted the absorption tail from 410 to 480 nm (see ESI,† Fig. S7). Obviously, the iodide anion engages in CT interactions with Py^+ ions in solutions and this is a known phenomenon.[24] Likewise, we have reported recently that green- or brown-colored Py^+ iodide crystals feature an additional red-shifted CTAB that is absent in SS absorption spectra of the corresponding colorless crystalline perchlorates, mesylates and chlorides.[8b,10a,b] Overall, our observations conform to the literature[24,25] showing the lack of CT between the Py^+ ion and perchlorates, chlorides and mesylates. Consequently, the CTI calculations were performed using aromatic cations.

Cationic luminophore **2a** features five electron and five hole transfer pathways, whereas **1**, **2b**, **3**, **4a** and **4b** have five, seven, five, nine and three electron and five, seven, five, nine and three hole transfer pathways, respectively (see ESI,† pageS S25–27). As an illustration, a dimer in the crystal lattice of **2a** is characterized by two (one red and one blue) inter-dimer pathways as well as by several other CTPs to adjacent molecules (the adjacent molecules have been omitted for clarity; see Fig. 4A). The effectiveness of each CTP was approximated by the intermolecular electronic coupling value V (see ESI,† page S28). Accordingly, higher absolute values of V ($|V|$) ensure a more plausible CT.

Having calculated $|V|$ values for each of the CTPs under consideration, we selected the most plausible hole and electron CTPs for **1–4** in the crystal lattice. Specifically, three major electron and three major hole CTPs with the highest $|V|$ values were selected for each luminophore. The sum of the electronic couplings $\Sigma|V|$ for the six (three for hole and three for electron) major CTPs was calculated to be 0.084, 0.119, 0.109, 0.295, 0.159 and 0.075 eV for **1**, **2a**, **2b**, **3**, **4a** and **4b**, respectively (Fig. 4B and 4C). Notably, the disregarded CTPs contributed less than 3% to the $\Sigma|V|$. Among multiple hole and electron CTPs that contributed to $\Sigma|V|$, one pathway for each of the luminophores had a disproportionately high $|V|$ value. These pathways were attributed to the intermolecular electrostatic π^+–π^+ interactions. Hence, the π^+–π^+ interactions contributed from 0% (in the absence of π^+–π^+ interactions for **4b**) to 25% (in **4a**), 38% (in **2b**), 59% (in **1**), 74% (in **2a**) and 96% (in **3**) of the total $\Sigma|V|$ (Fig. 4B). The disproportionately high contribution of the π^+–π^+ interaction CTP to the overall electronic communications highlights its importance in the crystal state CT processes.

Finally, the observed direct proportionality between calculated $\Sigma|V|$ and Φ values provided additional evidence for the key role of CT in the crystal state emission of **1**–**4**. Thus, the lowest Φ in the 17–20% range for **1** and **4b** correlated well with the lowest calculated $\Sigma|V|$ of 0.084 and 0.075 eV, respectively. The increased Φ for **2b** (35.0%), **2a** (43.5%) and **4a** (42.3%) nicely correlated with the higher $\Sigma|V|$ in the 0.100–0.160 eV range, while the highest $\Sigma|V|$ of 0.295 eV corresponded to the most emissive luminophore **3** (85.2%, Fig. 4C). Notably, the observed good correlation (R^2 = 0.95) between SS Φ and $\Sigma|V|$ values also provided evidence that counter ions such as mesylates, chlorides and perchlorates do not directly participate in the SS emission of Py^+ luminophores.

To verify the generality of our findings, we applied the SS CTI analysis for a series of highly planar Py^+ luminophores **15**–**17** of completely distinct design[10c] (see Fig. 4D). Gratifyingly, good correlation between the calculated $\Sigma|V|$ values and SS Φ was observed for **15**–**17**. Thus, the highest $\Sigma|V|$ value of 0.524 eV for **15** matched the highest solid state Φ of 88.5%. Likewise, the lowest $\Sigma|V|$ value of 0.179 eV was calculated for **17**, which featured poor Φ (19.6%; see ESI,† pages S35–S37 for details).

In conclusion, CTI analysis in combination with X-ray single crystal data has provided important insight into the emission mechanism of crystalline Py^+ salts and revealed the key role of intermolecular π^+–π^+ interactions in the SS photoluminescence. Thus, SS Φ was shown to be proportional to the TSCT intensity that was quantified by calculating the total electronic coupling ($\Sigma|V|$) value between luminophores in the crystal lattice. The π^+–π^+ interactions provide a disproportionately high (up to 96%) contribution to $\Sigma|V|$ between luminophore molecules. Hence, the π^+–π^+ interactions increase Φ for Py^+ luminophores by enhancing CT intensity. The CT between Py^+ moieties can be strengthened by TS electron donation from the electron-rich carbazole moiety to a Py^+ ring. The stronger π^+–π^+ interactions translated into a significant rise in the SS Φ from 17% to 85%. We believe that our findings on the role of electrostatic (π^+–π^+) interactions in CT emission phenomena will be instrumental in the design of emitters with outstanding photoluminescence properties both in solution and in the SS.

This work was funded by ERDF project No. 1.1.1.1/18/A/063. We thank Dr S. Belyakov for X-ray crystallographic analysis and M. Baumane for the synthesis of compound **2a**.

Conflicts of interest

There are no conflicts to declare.

Notes and references

1 (*a*) Y. Shirota, *J. Mater. Chem.*, 2000, **10**, 1–25; (*b*) V. Anand, R. Mishra and Y. Barot, *Dyes Pigm.*, 2021, **191**, 109390.
2 (*a*) K. Matsuki, P. Jiang and T. Taishi, *Adv. Funct. Mater.*, 2020, **30**, 1908641; (*b*) E. Fresta and R. D. Costa, *J. Mater. Chem. C*, 2017, **5**, 5643–5675.
3 (*a*) B. C. Thompson and M. J. F. Jean, *Angew. Chem., Int. Ed.*, 2008, **47**, 58–77; (*b*) R. O. Kesinro, A. O. Boyo, M. L. Akinyemi, M. E. Emetere and A. P. Aizebeokhai, *IOP Conf. Ser.: Earth Environ. Sci.*, 2021, **665**, 012036.
4 (*a*) S. Kawata and Y. Kawata, *Chem. Rev.*, 2000, **100**, 1777–1788; (*b*) W. Tang, Y. Huang, L. Han, R. Liu, Y. Su, X. Guo and F. Yan, *J. Mater. Chem. C*, 2019, **7**, 790–808.
5 H.-C. Gee, C.-H. Lee, Y.-H. Jeong and W.-D. Jang, *Chem. Commun.*, 2011, **47**, 11963–11965.
6 (*a*) M. Y. Wong and E. Zysman-Colman, *Adv. Mater.*, 2017, **29**, 1605444; (*b*) S. Mukherjee and P. Thilagar, *Chem. Commun.*, 2015, **51**, 10988–11003.
7 R. Katoh, K. Suzuki, A. Furube, M. Kotani and K. Tokumaru, *J. Phys. Chem. C*, 2009, **113**, 2961–2965.
8 (*a*) P. Xie, Y. Zhou, X. Li, X. Liu, L. Liu, Z. Cao, J. Wang and X. Zheng, *Chin. Chem. Lett.*, 2023, **34**, 107582; (*b*) K. Leduskrasts, A. Kinens and E. Suna, *Chem. Commun.*, 2019, **55**, 12663–12666; G. Zhang, X. Zhang, L. Kong, S. Wang, Y. Tian, X. Tao and J. Yang, *Sci. Rep.*, 2016, **6**, 37609.
9 (*a*) A. S. Klymchenko, *Acc. Chem. Res.*, 2017, **50**, 366; (*b*) S. A. Jenekhe and J. A. Osaheni, *Science*, 1994, **265**, 765.
10 (*a*) K. Leduskrasts and E. Suna, *RSC Adv.*, 2019, **9**, 460; (*b*) K. Leduskrasts and E. Suna, *RSC Adv.*, 2020, **10**, 38107; (*c*) X. Cui, Y. Hao, W. Guan, L. Liu, W. Shi and C. Lu, *Adv. Opt. Mater.*, 2020, **8**, 2000125.
11 X.-H. Jin, C. Chen, C.-X. Ren, L.-X. Cai and J. Zhang, *Chem. Commun.*, 2014, **50**, 15878–15881.
12 C.-X. Yuan, X.-T. Tao, Y. Ren, Y. Li, J.-X. Yang, W.-T. Yu, L. Wang and M.-H. Jiang, *J. Phys. Chem. C*, 2007, **111**, 12811–12816.
13 H.-L. Shen, P.-W. Hsiao, R.-H. Yi, Y.-H. Su, Y. Chen, C.-W. Lu and H.-C. Su, *Dyes Pigm.*, 2022, **203**, 110346.
14 E. Taipale, N. A. Durandin, J. K. Salunke, N. R. Candeias, T.-P. Ruoko, J. S. Ward, A. Priimagi and K. Rissanen, *Mater. Adv.*, 2022, **3**, 1703–1712.
15 W. Chen, S. A. Elfeky, Y. Nonne, L. Male, K. Ahmed, C. Amiable, P. Axe, S. Yamada, T. D. James, S. D. Bull and J. S. Fossey, *Chem. Commun.*, 2011, **47**, 253–255.
16 K. Leduskrasts and E. Suna, *ChemistryOpen*, 2021, **10**, 1081–1086.
17 S. Yamada, *Coord. Chem. Rev.*, 2020, **415**, 213301.
18 The placement of two luminophore fragments in spatial proximity is frequently used to enhance photoluminescence properties: (*a*) H. Tsujimoto, D.-G. Ha, G. Markopoulos, H. S. Chae, M. A. Baldo and T. M. Swager, *J. Am. Chem. Soc.*, 2017, **139**, 4894–4900; (*b*) C. Jiang, J. Miao, D. Zhang, Z. Wen, C. Yang and K. Li, *Research*, 2022, **2022**, 1–12; (*c*) T. Huang, Q. Wang, G. Meng, L. Duan and D. Zhang, *Angew. Chem., Int. Ed.*, 2022, **61**, e202200059; (*d*) D.-R. Bai, X.-Y. Liu and S. Wang, *Chem. – Eur. J.*, 2007, **13**, 5713–5723; (*e*) Y. Song, M. Tian, R. Yu and L. He, *ACS Appl. Mater. Interfaces*, 2021, **13**, 60269–60278; (*f*) H. Miranda-Salinas, Y.-T. Hung, Y.-S. Chen, D. Luo, H.-C. Kao, C.-H. Chang, K.-T. Wong and A. Monkman, *J. Mater. Chem. C*, 2021, **9**, 8819–8833.
19 CCDC 2216260, 2216261, and 2247114–2247116 contains the supplementary crystallographic data for luminophores 2–4.
20 C. Schäfer, M. Ruggenthaler, H. Appel and A. Rubio, *PNAS*, 2019, **116**, 4883–4892.
21 (*a*) A. A. Voityuk, *Phys. Chem. Chem. Phys.*, 2012, **14**, 13789; (*b*) C.-P. Hsu, *Acc. Chem. Res.*, 2009, **42**, 509–518.
22 (*a*) A. Benny, R. Ramakrishnan and M. Hariharan, *Chem. Sci.*, 2021, **12**, 5064–5072; (*b*) A. A. Voityuk, N. Rösch, M. Bixon and J. Jortner, *J. Phys. Chem. B*, 2000, **104**, 9740–9745; (*c*) Z. Q. You and C. P. Hsu, *Int. J. Quantum Chem.*, 2013, **114**, 102–115.
23 J. S. Brown, *Catnip (version 1.9)*, 2018. Available from **https://github.com/JoshuaSBrown/QC_Tools**.
24 E. M. Kosower and J. C. Burbach, *J. Am. Chem. Soc.*, 1956, **78**, 5838–5842.
25 Z.-X. Li, C.-H. Xu, W. Sun, Y.-C. Bai, C. Zhang, C.-J. Fang and C.-H. Yan, *New J. Chem.*, 2009, **33**, 853.
26 L. Jacob, E. Rzeszotarska, M. Koyioni, R. Jakubowski, D. Pociecha, A. Pietrzak and P. Kaszyński, *Chem. Mater.*, 2022, **34**, 6476–6491.

